Trends in ferromagnetism, hole localization, and acceptor level depth for Mn substitution in GaN, GaP, GaAs and GaSb

Priya Mahadevan and Alex Zunger

National Renewable Energy Laboratory, Golden 80401

(Dated: February 2, 2008)

Abstract

We examine the intrinsic mechanism of ferromagnetism in dilute magnetic semiconductors by analyzing the trends in the electronic structure as the host is changed from GaN to GaP, GaAs and GaSb, keeping the transition metal impurity fixed. In contrast with earlier interpretations which depended on the host semiconductor, we found that a single mechanism is sufficient to explain the ferromagnetic stabilization energy for the entire series.

PACS numbers: PACS number: 75.50.Pp,75.30.Et,71.15.Mb

Mn substitution on the Ga site of GaX III-V semiconductors with X=N, P, As and Sb creates a hole-producing acceptor level E(0/-) and renders the system ferromagnetic. Mean field models [1, 2, 3] aim to explain this effect by postulating that the Mn induced hole is a delocalized, host-like shallow acceptor (analogous to that introduced by Zn doping in GaAs) which couples to the localized S=5/2 magnetic moment of Mn. Since, however, it is now known that Mn in GaN introduces a *deep* ($\sim$ midgap) acceptor [4], with highly *localized* hole states [5, 6], a different mechanism needs to be invoked within previous approaches to explain ferromagnetism in nitrides [2] as opposed to arsenides. Using first-principles total-energy calculations of Mn in GaN, GaP, GaAs and GaSb, we show that, in fact, a single mechanism suffices to reveal systematic trends in the ferromagnetic stabilization energies in this entire series. The calculations reveal clear trends in (i) hole localization, (ii) acceptor level depth and (iii) ferromagnetic stabilization energy, all increasing along the GaSb $\rightarrow$ GaAs $\rightarrow$ GaP $\rightarrow$ GaN series. These trends reflect an enhanced coupling between p-d hybrids on different Mn sites along the series.

Experimentally, the trends along the GaX series are often clouded by growth-induced imperfections, including the formation of clusters [7], precipitates [8, 9], presence of anti-site defects [10] and non-substitutional impurity sites [11]. To clarify the *underlying intrinsic mechanism* of ferromagnetism (FM), we intentionally simplify the problem drastically, considering defect-free cases with only substitutional impurities. This approach reveals clear trends. In order to address the issues of trends, we have constructed 64 atom supercells of zinc-blende (ZB) GaN, GaP, GaAs and GaSb in which we replace one or two Ga atoms by Mn. The lattice constant of the Mn-containing supercells are taken from Ref. [6]. We have performed plane-wave pseudopotential total energy calculations [12] using the GGA exchange functional [13] as implemented in the VASP [14] code. We relaxed all atomic positions, calculating the total energy for the neutral and negatively charged state of Mn_{Ga} thus obtaining acceptor energies [6] E(0/-). In addition we calculated the total energy difference for two Mn spins aligned ferromagnetically and antiferromagnetically, determining the energy difference, E_{FM}-E_{AFM} - a measure of the stability of the ferromagnetic state.

Figure. 1 shows the calculated Mn d projected local density of states for neutral substitutional Mn in four ZB GaX compounds. The states are designated by t_2 or e to denote the symmetry of the representations that they correspond to, and by $+$ and $-$, to denote spin-up or spin-down respectively. The height of the peaks reflect the degree of localization

of the state within a sphere of radius 1.2 $\AA$ about the Mn site. We find a *pair* of t_2 states in each spin channel, reflecting bonding and antibonding states formed by the *p*-*d* interaction of Mn *d* states with host derived anion *p* states. The Fermi energy in all cases lies within the antibonding t_+ level, which in the neutral charge state of the impurity is partially occupied with two electrons (and therefore one hole). We see that while in GaN:Mn, the hole-carrying t_+^2 level is strongly Mn-localized, the degree of Mn-localization of the hole level decreases along the series GaN $\rightarrow$ GaP $\rightarrow$ GaAs $\rightarrow$ GaSb. This is seen also in Fig. 2 which depicts the wavefunction square of the antibonding t_+ state at E_F, evaluated at k=0. In contrast to what is expected from host-like-hole models [1, 2, 3], we find significant weight of the hole only on a unit comprising Mn and its nearest neighbors. This t_+ state has earlier been identified [6] as the antibonding state arising from *p*-*d* interactions between the Mn t_2(d) states with the corresponding t_2(p) states localized on the anion nearest neighbors. (The antibonding nature is evident from the pocket of zero charge density along the Mn-X bond). Concomitant with the reduced Mn localization on the *antibonding* t_+ state at E_F, the *bonding* state at 3-4 eV below the valence band maximum exhibits (in Fig. 1) increased Mn localization along the same GaN $\rightarrow$ GaP $\rightarrow$ GaAs $\rightarrow$ GaSb series (as a result of "*pd* level anticrossing" discussed in [6]).

By adding an electron to the antibonding t_+^2 level, we convert $Mn^{3+}(t^2)$ to $Mn^{2+}(t^3)$, thus creating an acceptor transition. The corresponding change E(0/-) in the total energy is depicted in Fig. 3 with respect to the calculated band edges [15] of the unstrained zincblende solids. We see that the acceptor level is very deep in GaN:Mn in agreement with experiment [4] and it becomes progressively shallower as the anion X becomes heavier, also in agreement with experiment [16]. Thus, moving along the series GaN $\rightarrow$ GaP $\rightarrow$ GaAs $\rightarrow$ GaSb, the *antibonding*, hole-carrying t_+ orbital becomes less Mn-localized, the acceptor level becomes shallower, and the bonding orbitals located inside the valence band become more localized on Mn, as observed in photoemission experiments [17]. The strong *d* character of the hole in Mn doped GaX semiconductors has implications on the usefulness of these materials as a source of spin-polarized carriers (ferromagnetic injectors in spintronic devices). For instance Mn in GaN has a deep acceptor level, which implies that it will not provide an easy source of holes to make GaN *p*-type.

To assess the ferromagnetic stability, we compute the energy difference E_{FM} - E_{AFM} between a ferromagnetic (FM) and an antiferromagnetic (AFM) spin arrangement on the

two Mn atoms in the supercell. The two Mn atoms are positioned at first, second, third and fourth fcc-neighbor positions (n=1,2,3,4 respectively); the corresponding Mn-Mn exchange interaction strengths versus n are depicted in Fig. 4. The trends in our calculations are consistent with what is found earlier [18]. Although the results shown in Fig. 4 suggest a more rapid decay of the exchange interaction strengths for GaN compared to GaAs, one finds that at fourth neighbor separation the interaction strengths are comparable in agreement with what is found in Ref. [19]. However, the structure more relevant to experiment is the wurtzite structure in the case of GaN. Recent theoretical calculations suggest [19] that the exchange interaction energies for Mn in wurtzite GaN fall off more rapidly with distance than in the zincblende structure. We see

1. Strong FM stabilization in GaN:Mn, despite the fact that the hole orbital is a highly localized (Figs. 1,2), deep acceptor (Fig. 3) state. Even though our conclusion that GaN:Mn shows large ferromagnetic stabilization energies for some pairs of Mn atoms parallels that of Dietl and Ohno [2], the mechanism behind it is entirely different: Their model assumes a host-like delocalized hole for all materials, on the basis of which they attributed trends in J to *volume scaling*, $J \sim V^{-1}$=R^{-3}, leading to a large J for the shortest bond-length material (here, GaN). We allow different materials to exhibit different localizations, finding large FM stabilization energies in GaN *despite* it not having host-like-hole states. Consistent with the deeper acceptor level for GaN:Mn (Fig. 3) and its more localized hole-carrying orbital (Fig. 2), it's spin-spin interaction is shorter-ranged (viz. 2nd and 3rd neighbors in Fig. 4).

2. The exchange interaction strengths are large even for fourth neighbor Mn pair separations (Fig. 4). Thus, *indirect* exchange (via the intervening anions) is at play.

3. Certain crystallographic orientations of the Mn-Mn pair are seen to have the largest stabilization energies for the ferromagnetic state, e.g. the <110> orientation akin to n=1 and n=4 neighbors, whereas <001>-oriented pairs (n=2) have the weakest FM. This reflects the orientational dependence of the coupling matrix elements between the two t_2 (pd) hybrids orbitals located on different Mn sites. The matrix elements and therefore the bonding is maximized when the t_2 (pd) hybrid orbitals point towards each other. On the other hand in zincblende symmetry e-orbitals point $in-between$ the nearest neighbors, leading to vanishing matrix elements when the Mn atoms occupy <110> oriented lattice positions. Indeed there can be several exchange paths, between the t_2 orbitals on the two Mn atoms, the most obvious choice being one mediated via the host anion states *via* p-d coupling, and

the other mediated by d-d interaction. Our calculations help us distinguish which is the relevant exchange path. For cases where the hole is in a level with e symmetry, such as GaAs:Fe− [6], the ferromagnetic contribution from the hole is found to be small. As the coupling to the host is absent for a hole with e symmetry, this suggests that the relevant exchange path in these systems is *via* p-d coupling mediated by the host semiconductor states.

4. We conclude that the p-d interaction couples the d levels on Mn ion to the p-like dangling bond states of the Ga vacancy, thus creating p-d hybrids localized on Mn and its neighbors. The interaction of such partially occupied t_+^2 orbitals between different Mn sites stabilizes FM. The chemical trends in localization (Fig.2), acceptor energies (Fig. 3) and the exchange interaction strengths (Fig. 4) reflect the position of the Mn d orbital energies relative to the host band edges.

We acknowledge support from the Office of Naval Research.

---

[1] T. Dietl, H. Ohno, F. Matsukura, J. Cibert and D. Ferrand, Science **287**, 1019 (2000).

[2] T. Dietl, Semicon. Sci. and Tech. **17**, 377 (2002).

[3] T. Dietl, F. Matsukura, and H. Ohno, Phys. Rev. B **66**, 033203 (2002); J. König, J. Schiemann, T. Jungwirth and A.H. MacDonald, in *Electronic Structure and Magnetism of Complex Materials*, edited by D.J. Singh and D.A. Papaconstantopoulos, Springer verlag (2002).

[4] T. Graf, M. Gjukic, M.S. Brandt, M. Stuzmann, and O. Ambacher, Appl. Phys. Lett. **81**, 5159 (2002).

[5] M. van Schilfgaarde and O.N. Mryasov, Phys. Rev. B **63**, 233205 (2001).

[6] P. Mahadevan and A. Zunger, Phys. Rev. B **69**, 115211 (2004).

[7] S. S. A. Seo, M. W. Kim, Y. S. Lee, T. W. Noh, Y. D. Park, G. T. Thaler, M. E. Overberg, C. R. Abernathy and S.J. Pearton, Appl. Phys. Lett. **82**, 4749 (2003).

[8] S. Dhar, O. Brandt, A. Trampert, L. Daweritz, K.J. Friedland, K.H. Ploog, J. Keller, B. Beschoten, G. Guntherodt, Appl. Phys. Lett. **82**, 2077 (2003).

[9] F. Matsukura, E. Abe, Y. Ohno and H. Ohno, Appl. Surf. Sc. **159-160**, 265 (2000).

[10] B. Grandidier, J.P. Nys, C. Delerue, D. Stievenard, Y. Higo and M. Tanaka, Appl. Phys. Lett. **77**, 4001 (2000).

[11] K.M. Yu, W. Walukiewicz, T. Wojtowicz, I. Kuryliszyn, X. Liu, Y. Sasaki, and J.K. Furdyna, Phys. Rev. B **65**, 201303 (2002).

[12] J. Ihm, A. Zunger and M.L. Cohen, J. Phys. C:**12**, 4409 (1979).

[13] J.P. Perdew and W. Wang, Phys. Rev. B **45**, 13244 (1992).

[14] G. Kresse and J. Furthm*ü*ller, Phys. Rev. B. **54**, 11169 (1996); G. Kresse and J. Furthm*ü*ller, Comput. Mat. Sci. **6**, 15 (1996).

[15] S.H. Wei and A. Zunger, Appl. Phys. Lett. **72**, 2011 (1998).

[16] J. Schneider in *Defects in Semiconductors II, Symposium Proceedings*, Edt. S. Mahajan and J.W. Corbett, 225 (North-Holland, 1983); B. Clerjaud, J. Phys. C **18**, 3615 (1985).

[17] J. Okabayashi, A. Kimura, O. Rader, T. Mizokawa, A. Fujimori, T. Hayashi and M. Tanaka, Phys. Rev. B **58**, 4211 (1999).

[18] K. Sato, P.H. Dederics and H. Katayama-Yoshida, Europhys. Lett. **61**, 403 (2003).

[19] J. Kang, K.C. Chang and H. Katayama-Yoshida, J. Superconductivity (in press).

FIG. 1: Mn d projected partial density of states for a single Mn in ZB GaN, GaP, GaAs and GaSb, where the symmetry (t_2 and e) as well as the spin (+ and -) have been indicated. The shaded region represents the t_2^+ states.

FIG. 2: Wavefunction squared plots of the hole wavefunction taken at Γ point for Mn in the <110> plane of ZB GaN, GaP, GaAs and GaSb. The lowest contour (blue) represents 0.015 e/A^3 and the maximum contour (red) have been chosen so that the integrated charge density is 90%. Mn (Ga) atoms have been indicated by filled (open) black circles, while anion atoms are represented by filled red circles.

FIG. 3: Calculated acceptor levels Mn(0/-) in III-V's. The host band edges are aligned according to the calculated unstrained band offsets [15].

FIG. 4: Calculated exchange interaction strengths between Mn atoms occupying 1st, 2nd, 3rd and 4th fcc-neighbor positions in a zincblende lattice of GaN, GaP, GaAs and GaSb respectively.

This figure "fig1.jpg" is available in "jpg" format from:

http://arXiv.org/ps/cond-mat/0409296v1

This figure "fig2.jpg" is available in "jpg" format from:

http://arXiv.org/ps/cond-mat/0409296v1

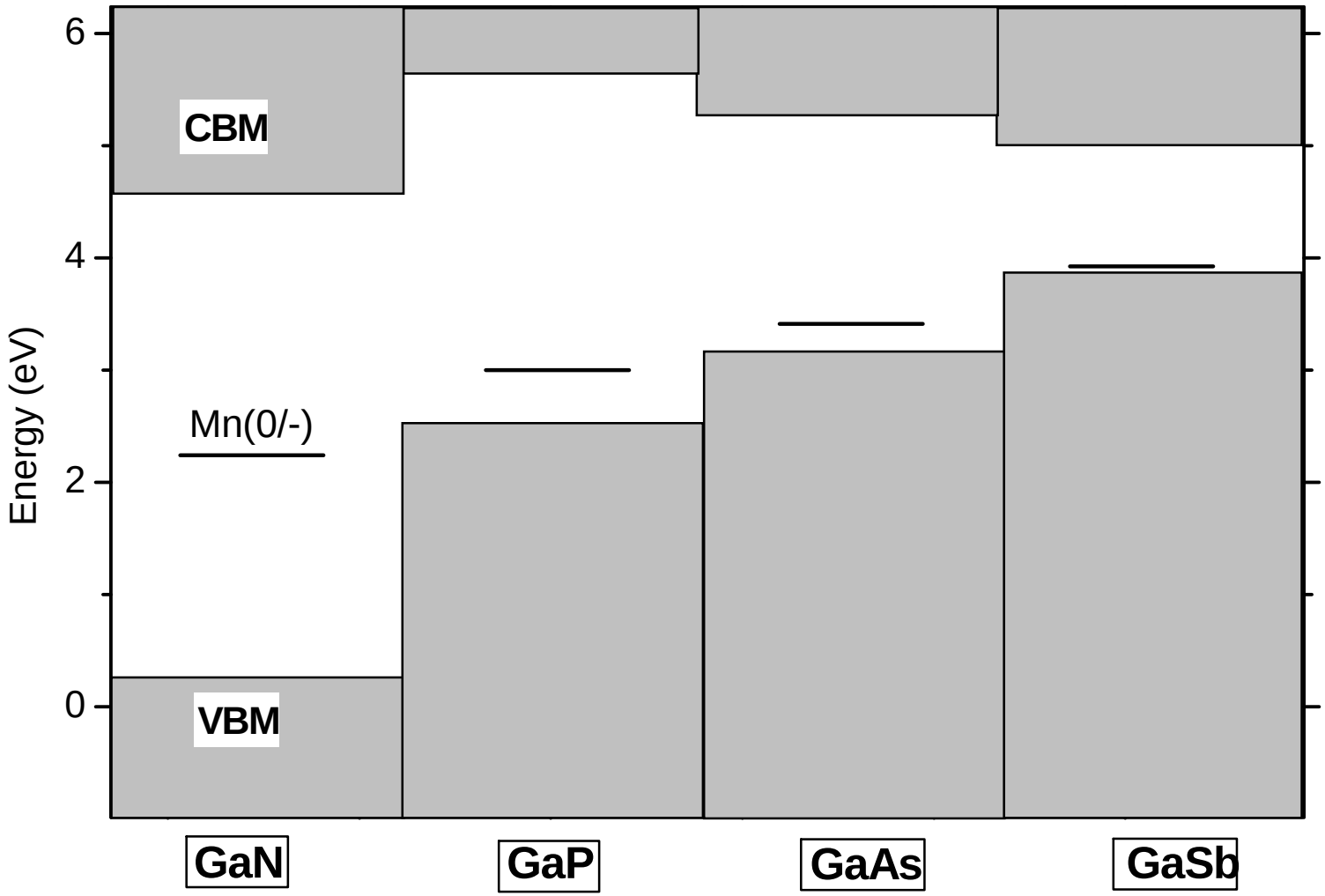

Fig. 3
Mahadevan and Zunger

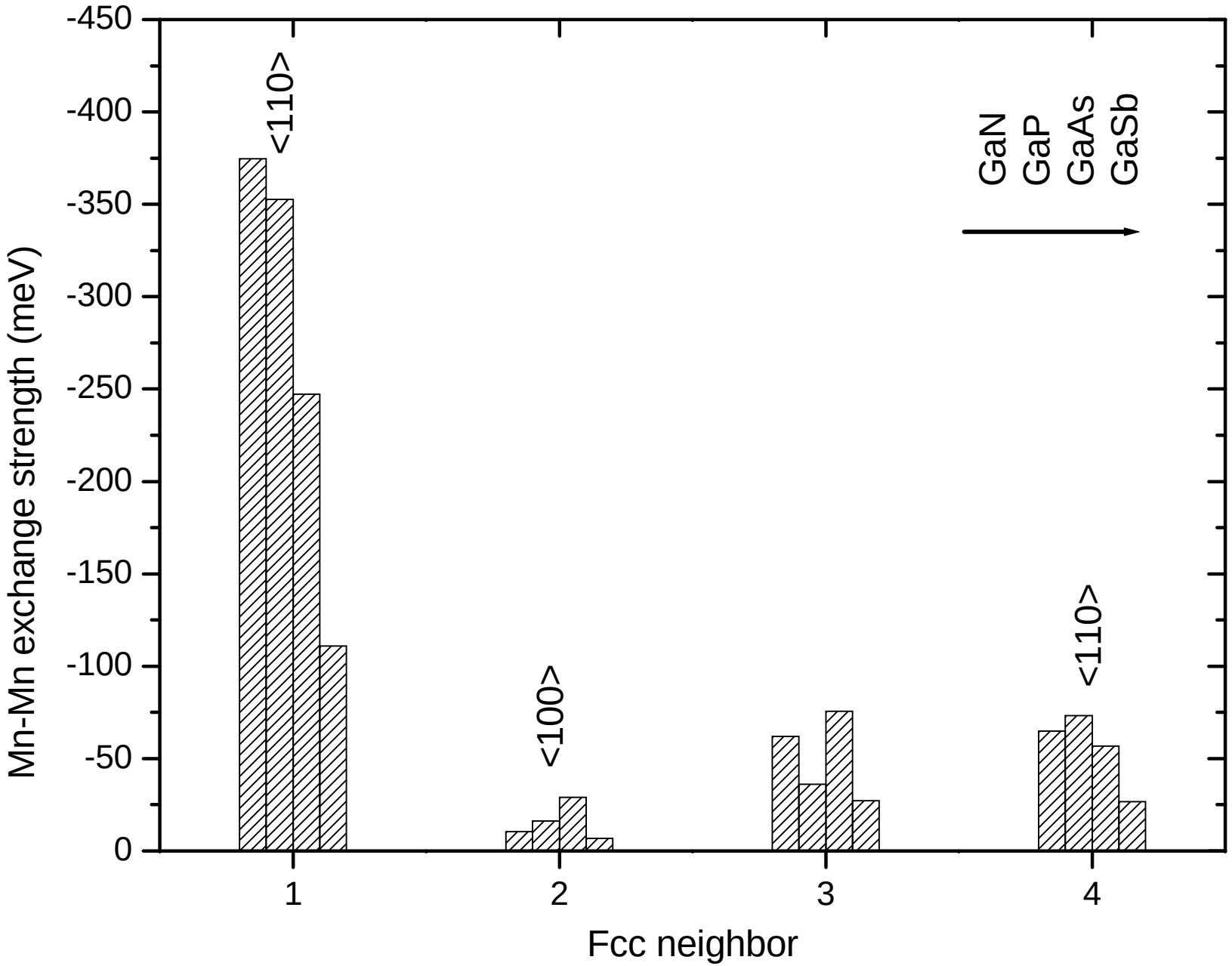

Fig. 4
Mahadevan and Zunger